

KIL 12023
Copy 2 R61
ACCN: 215080

RAL-92-023 Science and Engineering Research Council

Rutherford Appleton Laboratory

Chilton DIDCOT Oxon OX11 0QX

RAL-92-023

***** RAL LIBRARY R61 *****
ACC_No: 215080
shelf: RAL 92023
R61

Nonlinear Response Function Estimation III: Analysis of a Nonlinear RLC Electrical Resonator Circuit

T Dewson A D Irving and N H Cunliffe

LIBRARY, R61
-1 JUN 1992
RUTHERFORD APPLETON
LABORATORY

April 1992

Science and Engineering Research Council

"The Science and Engineering Research Council does not accept any responsibility for loss or damage arising from the use of information contained in any of its reports or in any communication about its tests or investigations"

NONLINEAR RESPONSE FUNCTION ESTIMATION III : ANALYSIS OF A NONLINEAR RLC ELECTRICAL RESONATOR CIRCUIT

T Dewson* , AD Irving⁺ and NH Cunliffe⁺

* Department of Mechanical Engineering, Queen's Building, University Walk,
University of Bristol, Bristol, BS8 1TR, UK.

+ Rutherford Appleton Laboratory, Chilton, Didcot, Oxon, OX11 0QX, UK.

ABSTRACT

In this work, a formalism for the estimation of the response functions from a mixed order (linear + non-linear) system, recently developed by the authors and presented in companion papers, is employed to identify the response functions of a non-linear electrical resonator circuit. Electrical resonator circuits of the type used in this work have previously been employed to investigate the period doubling route to chaos and the experimental verification of theoretically predicted universal constants. In this work we follow the same experimental procedure of these previous investigators. First and second order response functions are estimated from the time series of the driving voltage and the voltage across the LC components, collected from the circuit. These estimated response functions are then employed to predict the voltage across the LC components of the circuit, for a range of different driving frequencies and voltage amplitudes for a sinusoidal input signal, and for a random noise input signal. This work demonstrates that a single set of response functions can characterise a wide area of the phase space of the circuit, and so also demonstrates the applicability of the input-output representation, known as the Volterra series, to a wide class of systems which exhibit non-linear phenomena.

INTRODUCTION

There exists a considerable amount of work in the literature on the effects of non-linearity in physical systems. However, the detailed analysis of the experimental time series from nonlinear systems remains an outstanding problem. Consequently this is an important issue, which has an impact in many areas of science and engineering. Most of the techniques that are currently employed to analyse data from these systems are based on the methods developed for the analysis of time series data from linear systems, for example, the linear correlation function, and its Fourier transform, the spectral density. Even though techniques exist that can estimate the non-linear terms, these require stringent approximations in order to simplify the analysis. For instance in maximum likelihood methods, the order and form of the model must be selected before the analysis commences, as the number of parameters that may be fitted is severely limited.

It has long been known that for a linear time-invariant system the first order impulse response function represents a complete description of the phenomenon. This representation is based upon a characterisation of the physical system in terms of its observables. It is equally important to realise that for many non-linear phenomena a set of non-linear response functions also offer a complete description of the physical process. The generalisation of the well known linear convolution equation is known as the Volterra series [1,2], first employed by Wiener [3,4] to characterise the input-output behaviour of non-linear systems. In this generalisation, the causal relationship between the input time series $\{x(t)\}$ and the output time series $\{y(t)\}$ is expressed in terms of a set of response functions $\{h_i(\tau_1, \dots, \tau_i), i=1,N\}$, where N and μ are, respectively, the order and the finite length of the memory, of the non-linear process, and may be written, for discrete data as,

$$y(t) = \sum_{n=1}^N \frac{1}{n!} \sum_{\tau_1=0}^{\mu} \dots \sum_{\tau_n=0}^{\mu} h_{x\dots xy}(\tau_1, \tau_2, \dots, \tau_n) \prod_{i=1}^n x(t-\tau_i) \quad (1)$$

This is an input-output 'black box' representation of a system, where the response functions or Volterra kernels, $h_n(\tau_1, \tau_2, \dots, \tau_n)$, characterise the system, and where t denotes time and the τ_i 's denote time delay with respect to the time t . The values of the Volterra kernels represent those finite amplitude finite memory impulse response functions that describe the nonlinear system in terms of its physical observables, and are linked to the usual internal description approach, for example in the form of differential equations, through the realisation process. This characterisation is a localized model which interrelates the instantaneous voltages to the response or time averaged Green's functions of the circuit. It is a localized model in that a point, in the phase space, was selected and the nonlinear properties of the circuit, at that point, estimated. These nonlinear relationships were then used to predict the behaviour of the circuit at other points in the phase space of the circuit. In principle a global model may be estimated at any given point, however this is not usually done in practice.

In the first two papers of this series [5,6], a formalism was developed for the estimation of the non-linear response functions from an analysis of the experimental time series data for the mixed [5] and isolated [6] order cases. This formalism overcomes the need to use the delta functional approximations that have previously been applied to simplify the multi-dimensional convolution integrals, in order to analyse time series from non-linear systems. These include the use of special input sequences, for example a sinusoidal input or white noise, or the direct interaction approximation (i.e the response functions between modes are assumed to be of a dirac delta functional form), applied to turbulent flow by Kraichnan [7]. In this work, this formalism is applied to analyse the properties of an electronic resonator circuit, which displays both non-linear and chaotic behaviour.

Non-linear electrical resonators are known to be a valuable means to experimentally investigate the properties of dynamic non-linear systems, due to the simplicity of the system and the richness of the observed behaviour [8]. Circuits of this type have been used to compare the measured universal scaling parameters and the order of appearance of periodic windows from within chaos [8,9], with those predicted by theory [10]. Other investigators have experimentally determined 'phase diagrams' [11,12], in which the distinct responses of the resonator are associated with different 'phases' or regions of the phase space. In these experiments the circuit has been driven with periodic functions close to the resonant frequency of the circuit. In this paper we report a set of response function values, determined by our formalism, of an electrical resonator circuit using periodic driving functions.

EXPERIMENT

The non-linear resonator circuit analysed in this work is a series array of a resistor, inductor and capacitor (RLC), in which the capacitor, a Motorola MV2108 varactor diode, is the non-linear component. This diode has a non-linear charge-voltage characteristic as its capacitance varies as a function of the voltage across it. The resonator was driven, first sinusoidally by a AIRMEC 304 frequency synthesizer with a output impedance of 50Ω , and secondly by a CEL Instruments 213 random noise generator. The voltage across the capacitor and inductor components was considered as the output of the circuit, as in previous experiments using a circuit of this type [8,12], and was recorded using a Gould DSO1604 20 MHz oscilloscope. The resonator circuit was as shown in reference [8], and the values of the component used were, the resistance 180Ω , the inductance $120\mu\text{H}$ and the capacitance of the diode is given by equation (2). An analysis was performed on this output signal in the frequency domain using a linear spectral analyzer. The time series voltage across the LC components, along with the time series of the driving voltage signal to the circuit, were monitored by the Gould digital storage oscilloscope. The use of this digital storage oscilloscope enabled samples of the time series of the input and output signals to be collected, and downloaded to a Personal Computer (PC). The downloaded time series in

binary format, from each experiment, were then converted to ASCII format and transferred to a Cray X/MP-416 for analysis.

At low drive voltages the circuit behaved as a linear RLC circuit, as the drive voltage was increased, the circuit displayed the frequency multiplications observed by previous investigators [8,9,12]. As in previous investigations the bifurcation mode or 'phase' could be determined from displaying the drive voltage versus the output signal on the oscilloscope in the x-y mode and from the power spectral density of the time series displayed on the spectral analyser. The Lissajou figures displayed on the oscilloscope contained a number of loops equal to the bifurcation mode or 'phase' excited. Once a particular bifurcation mode had been established, the real time input and output voltage signals were then captured by the digital oscilloscope, stored on the PC, transferred and analysed using the formalism, to estimate the linear and non-linear response functions of the resonator circuit.

BACKGROUND THEORY

The variactor diode which is the nonlinear element of the circuit has a capacitance which varies as a function of the voltage across it, such that under reverse voltage, the voltage across the diode, V_c , is given by,

$$V_c = \frac{q}{C(V_c)}$$

where the capacitance $C(V_c)$ is,

$$C(V_c) = \frac{C_o}{(1 - V_c/\phi)^\mu} \quad (2)$$

where $C_o = 80\text{pF}$, $\phi = 0.6\text{V}$ is the contact potential, and μ is the junction gradient, which varies from 0.5 for an abrupt junction to 0.33 for a graded junction. Under forward voltage, the variactor behaves like a normal conducting diode.

The equation governing the circuit can be considered to be roughly that of a damped harmonic oscillator [15],

$$\frac{d^2q}{dt^2} + a(q) \frac{dq}{dt} + f(q) = V_d(t)$$

where $a(q)$ and $f(q)$ are, respectively, the nonlinear damping and restoring forces of the circuit, and where $V_d(t)$ is the driving voltage. The motion of the charge carriers in the diode can be thought of as being analogous to a very soft elastic system with dissipation, thus as the system is driven harder, either by increasing the amplitude or frequency, their motion becomes locked into a sequence of sub-harmonics of the frequency of the drive voltage. These bifurcations represent the states which dissipate the minimum amount of energy for the system. At the end of the bifurcation sequence is the onset of chaos which is suggested to have a nonstationary and unstable family of chaotic solutions [14]. This implies that different regions of the phase space are governed by different families of solutions each with its own

equations of motion. In this scenario there is no global solution to the motion of the charge carriers.

It has also been suggested by various authors [8,9,11,12,15] that the successive extrema of the observed voltages may be modelled by a nonlinear return map of the form,

$$x_{n+1} = f(x_n, p) - Jx_n \quad (3)$$

where p is a set of parameters that can be determined empirically from the data, and J is a determinant which corresponds to the dissipation per cycle, and when $J \neq 0$ then the system may experience hysteresis [15]. Equation (3) is a nonlinear map between successive extrema of the sequence and assumes there is no noise in the process. Equations of this form may be readily solved [16], however there is noise in all experimental situations, and the return map should be written as,

$$x_{n+1} = f(x_n, p) - Jx_n + r_{n+1}$$

where $\{r(t)\}$ is a stochastic distribution. This is a form of nonlinear auto-regression [16], and there is no unique solution for the empirically devived parameters, p , because of the inclusion of the unknown $\{r(t)\}$ into the equation. Thus the estimated parameter values, p , will be dependant upon the choice of the properties of $\{r(t)\}$.

There is an alternative approach where the equation of motion of the charge carriers in the diode are governed by a sequence of nonlinear pulses or solitons [17], which propagate through the diode. The equation of motion thus becomes [18],

$$\frac{d^2q}{dt^2} + a(q) \frac{dq}{dt} + (e^q - 1) = \frac{V_d(t)}{\phi} \quad (4)$$

where r is the damping constant, and $(e^q - 1) (= \sum \alpha_i^2 \text{sech}^2(\alpha_i t - \beta_i k))$ is a sequence of pulses generated by $V_d(t)$. Equation (4) represents a description of the global behaviour of the diode, including the observed hysteresis effects, rather than the localised behaviour offered by the bifurcation and return map approaches.

If a global solution exists, then it should be possible to measure the properties of the system at a single point in the phase space, and then to employ these properties within other regions of the phase space. In this work we shall test this hypothesis by estimating the nonlinear response functions of the system at fully developed chaos and then observe whether or not these values can predict the behaviour of the circuit in the linear and the bifurcations regions.

THEORY OF ANALYSIS FORMALISM

In the first two papers of this series [5,6] a formalism has been developed for the estimation of the linear and non-linear response functions from an analysis of the input and output time series data of a system. This formalism is based upon the time delayed statistical moments, between the input and output time series, which are estimated from the

experimental data. These time series moments are used as the basis of a set of simultaneous equations, which relate these time delayed moments and the unknown response functions. This set of simultaneous inhomogeneous equations is solved algebraically for the unknown response function values of the physical process under study.

In this application of the new formalism, the sinusoidal drive voltage time series will be denoted by $V_i(t)$, and the output voltage by $V_o(t)$, and the equation relating the two, assuming that the system is causal, time-invariant and has a finite length memory, will be given by a Volterra series of the form,

$$V_o(t) = \sum_{n=1}^N \frac{1}{n!} \sum_{k_1=0}^{\mu} \dots \sum_{k_n=0}^{\mu} h_n(k_1, k_2, \dots, k_n) \prod_{i=1}^n V_i(t-k_i)$$

where N is the finite order of the system, μ is the length of the 'memory' of the system, and $h_n(k_1, k_2, \dots, k_n)$ is the n th order response function between the input and output voltages. The set of simultaneous equations constructed using the formalism [5] is given by,

$$M_{V_i \dots V_i V_o}(\tau_1, \dots, \tau_r) = \sum_{n=1}^N \frac{1}{n!} \sum_{k_1=0}^{\mu} \dots \sum_{k_n=0}^{\mu} h_n(k_1, \dots, k_n) M_{V_i \dots V_i V_i \dots V_i}(\tau_1, \dots, \tau_r, k_1, \dots, k_n) \quad (5)$$

for $r = 1, \dots, N$

where $M_{V_i \dots V_i V_o}(\tau_1, \dots, \tau_r)$ is the time delayed r th order cross moment between the $V_i(t)$ and $V_o(t)$ time series, and $M_{V_i \dots V_i V_i \dots V_i}(\tau_1, \dots, \tau_r, k_1, \dots, k_n)$ is the time delayed $(r+n)$ th order auto moment of the $V_i(t)$ time series. In this work we shall be using an absolute moment form in the calculation of the time series moments from the data, it has been shown that the analysis formalism is independent of the type of time series moment used, i.e absolute, central, etc [13]. This set of simultaneous equations may be written in the following matrix form as [5],

$$\begin{vmatrix} M_{V_i V_o}(\tau_1) \\ M_{V_i V_i V_o}(\tau_1, \tau_2) \\ \vdots \\ M_{V_i \dots V_i V_o}(\tau_1, \dots, \tau_N) \end{vmatrix} = \begin{vmatrix} M_{11} & M_{12} & \dots & M_{1N} \\ M_{21} & M_{22} & \dots & M_{2N} \\ \vdots & \vdots & \ddots & \vdots \\ M_{N1} & M_{N2} & \dots & M_{NN} \end{vmatrix} \begin{vmatrix} h_1(k_1) \\ h_2(k_1, k_2) \\ \vdots \\ h_N(k_1, \dots, k_N) \end{vmatrix} \quad (6)$$

where $M_{rs} = M_{V_i \dots V_i V_i \dots V_i}(\tau_1, \dots, \tau_r, k_1, \dots, k_s)$. This set of equations can be solved for the unknown response function values using standard matrix methods.

When applying the formalism it is necessary to choose suitable values for the order of the system (N) and the length of memory of the system (μ). As the circuit is described by a second order differential equation [8,9], it is reasonable to assume that the order of the system is two (i.e $N=2$), through the homogeneous replacement of the differential terms [2]. Figures 1 and 2 show a typical 100 points of time series data of the input to and the output from the circuit, when the circuit is driven by a random noise source (figure 1) and a frequency synthesizer, set at 1.95 MHz (figure 2). It can be observed from these figures that,

as the two signals are very similar in form, it can be assumed that the circuit has only a memory, which is short compared to the data sampling interval (50 ns).

Assuming that the system relating the input drive voltage, $V_i(t)$, and the output voltage, $V_o(t)$, can be described by a Volterra series of order two ($N=2$), having a short term finite memory, μ . Thus the equation relating the input and output voltages will be given by,

$$V_o(t) = \sum_{k_1=0}^{\mu} h_1(k_1) V_i(t-k_1) + \sum_{k_1=0}^{\mu} \sum_{k_2=0}^{\mu} h_2(k_1, k_2) V_i(t-k_1) V_i(t-k_2) \quad (7)$$

The set of simultaneous equations, which can be solved for the unknown response function values, are formed, from equation (5), such that matrix equation (6) becomes,

$$\begin{vmatrix} M_{V_i V_o}(\tau_1) \\ M_{V_i V_i V_o}(\tau_1, \tau_2) \end{vmatrix} = \begin{vmatrix} M_{V_i V_i}(\tau_1, k_1) & M_{V_i V_i V_i}(\tau_1, k_1, k_2) \\ M_{V_i V_i V_i}(\tau_1, \tau_2, k_1) & M_{V_i V_i V_i V_i}(\tau_1, \tau_2, k_1, k_2) \end{vmatrix} \begin{vmatrix} h_1(k_1) \\ h_2(k_1, k_2) \end{vmatrix} \quad (8)$$

with $0 \leq \tau_1 \leq \mu$, $0 \leq \tau_2 \leq \mu$, $0 \leq k_1 \leq \mu$, $0 \leq k_2 \leq \mu$, where $M_{V_i V_o}(\tau_1)$ and $M_{V_i V_i V_o}(\tau_1, \tau_2)$ are, respectively, the first and second order cross moments between the input and output voltage time series, $M_{V_i V_i}(\tau_1, k_1)$, $M_{V_i V_i V_i}(\tau_1, k_1, k_2)$ (and $M_{V_i V_i V_i}(\tau_1, \tau_2, k_1)$) and $M_{V_i V_i V_i V_i}(\tau_1, \tau_2, k_1, k_2)$ are, respectively, the second, third and fourth order auto moments of the time series of the input voltage, and $h_1(k_1)$ and $h_2(k_1, k_2)$ are, respectively, the unknown first and second order response functions.

The ability of the technique to correctly determine the response of the system will be demonstrated by displaying the predictive power of the estimated response functions, using equation (7), over a range of input voltages and frequencies. The predictive power of the model will be demonstrated by two test statistics, the root mean square (rms) difference and the normalised root mean square (nrms) difference between the measured and model predicted output voltage, where the RMS difference is given by

$$\text{rms} = \left[\frac{1}{T} \sum_{t=1}^T [y(t) - y_p(t)]^2 \right]^{1/2} \quad (9)$$

and the normalised RMS difference by,

$$\text{nrms} = \left[\frac{1}{T} \sum_{t=1}^T \left[\frac{y(t) - y_p(t)}{y(t)} \right]^2 \right]^{1/2} \quad (10)$$

ANALYSIS OF EXPERIMENTAL DATA

In this section, a set of response functions will be estimated, using the formalism recently developed by the authors [5], for the electrical resonator circuit, described in a previous section. The set of estimated response functions which characterise the system in terms of the physical observables, and this characterisation will then be used to test the

hypothesis that the response functions can accurately predict the circuit's behaviour over a wide range of the 'phases' exhibited by the resonator circuit. Electrical resonator circuits of this form have been reported to display non-linear behaviour, and have been used to investigate the period doubling route to chaos. In this work we have followed the experimental procedure of previous workers, so that the voltage across the capacitor and inductor components was monitored as the output of the circuit [8,12]. However in this work, as well as using a spectral analyser to identify particular states of the circuit, the output signal and the input drive voltage, were captured using a digital storage oscilloscope.

The frequency of the input signal was set at 1.95 MHz, and figure 2 shows a typical 100 points of the input and output voltage time series. The result of the analysis of this output time series using the spectral analyser is shown in figure 3. It can be observed that, at this drive voltage and frequency, the circuit is manifesting a form of the previously reported 'chaotic' behaviour displayed by this type of circuit. The time series sequence of the output signal recorded at 1.95 MHz, shown in figure 2, appears to be a non-stationary modulated sine wave rather than a stochastic or chaotic sequence. The time series auto and cross moments of varying orders are estimated from a 1000 point sample of this time series data set, and from these the first and second order response functions can be determined by the solution of equation (8), using standard matrix methods. The values of the response function estimates are given in Table 1,

Table 1 : Estimated First and second order response function values

	$k_1=0$	$k_1=1$
$h_1(k_1)$	0.9559	0.01363
$h_2(k_1,k_2)$	$k_1=0$	$k_1=1$
$k_2=0$	0.03728	-0.03004
$k_2=1$	-0.03004	0.03792

By using the estimated first and second order response function values, shown in table 1, and equation (7), it is possible to demonstrate the ability of the model estimated by the technique to predict the output voltage of the circuit, $V_{op}(t)$, given the driving voltage, $V_i(t)$. In the first example of this methodology, the ability of the estimated response functions to characterise the same operating region of the phase space, i.e fully developed chaos, from which the response functions had been estimated, will be demonstrated. A separate 100 point sample of the data set shown in figure 2 was chosen, and the estimated response functions and the driving voltage employed to predict the output voltage of the circuit, using equation (7). Figure 4 shows the observed and predicted (by the estimated response functions) output voltage from the circuit for this sample of data. A good agreement between the measured and

model predicted voltage can be observed to have been achieved, this is also confirmed by the values of the two test statistics, the rms and the normalised rms difference between the two time series are 0.318 and 1.398, respectively.

The above example has demonstrated the formalisms ability to predict the behaviour of the circuit at the same operating point in the phase space. In the following examples, the formalisms ability to predict the behaviour of the circuit at other operating points will be considered. This will determine whether or not, a global solution for the motion of the charge carriers exists, through the existence of a global model that can predict the behaviour of the circuit, across a range of driving voltages and frequencies.

In the other examples, the ability of the model described by the set of estimated response functions, to characterise a different 'phase' or bifurcation mode exhibited by the circuit will be demonstrated. In the second example the frequency of the input signal was changed to 1.79 MHz, where the circuit exhibited period x16 bifurcations, as can be observed in the spectral density shown in figure 5, which shows the characteristic signature of the x2, x4, x8 and x16 bifurcations. The spectral density of the x16 bifurcation state, shown in figure 5, may be qualitatively compared to the spectral density obtained at 'fully developed chaos', as shown in figure 3. The total area under the peaks of the spectrum is proportional to the power provided by the forcing function to maintain the motion of the charge carriers. As can be observed the area under the chaotic spectrum is greater than the sum of the areas under the sequence of bifurcation peaks. This is also true for the bifurcation sequences in the region of chaos and to the reverse bifurcation sequences beyond chaos. Qualitatively, this implies that the bifurcation states are energetically favorable to the motion of the charge carriers, whilst additional energy must be dissipated in the wave-wave or pulse-pulse interactions of the chaotic motion. Figure 6 shows the observed and predicted output voltage from the circuit, and again a good agreement can be observed. The value of the rms and normalised rms difference in this example are 0.444 and 0.248, respectively.

In the third example the frequency of the input driving signal was reduced to 1.73 MHz, where the circuit exhibited period x4 bifurcations. In the process of reducing the frequency of the driving signal, the bifurcation mode or 'phases' of period x8 was observed, on the spectral analyser, so indicating the bifurcation route to chaos. Figure 7 shows the observed and predicted output voltage from the circuit, when driven with at a frequency of 1.73 MHz, and again a good agreement can be observed. The value of the rms and normalised rms difference in this example are 0.484 and 0.623, respectively.

In the fourth example, the frequency of the input signal was reduced to 1 MHz, and in the process of reducing the frequency of the driving signal, the bifurcation mode or 'phases' of period x2 was observed, on the spectral analyser, which can be observed in the spectral

density shown in figure 8. Figure 9 shows the observed and predicted output voltage from the circuit, when driven with at a frequency of 1 MHz, and again a good agreement can be observed. The value of the rms and normalised rms difference in this example are 1.323 and 3.401, respectively.

In the final sinusoidal example, the amplitude of the driving voltage was reduced by a factor 10. Figure 10 shows the observed and predicted output voltage from the circuit, when driven with at a frequency of 1 MHz, and again a good agreement can be observed. The value of the rms and normalised rms difference in this example are 0.092 and 0.997, respectively.

Wiener, who was the first to characterise the input-output behaviour of non-linear systems in terms of the non-linear response functions and the Volterra series [3,4], indicated that the correct probe for non-linear systems was 'Gaussian white noise' rather than harmonic sequences. Hence for the final example, the frequency synthesizer used in the previous examples was replaced by the noise source. A sample of the input and output time series for this example can be observed in figure 1. Figure 11 shows the observed and predicted output voltage from the circuit, when driven with random noise source, again a good agreement can be observed. The value of the rms and normalised rms difference in this example are 0.027 and 2.318, respectively. This example demonstrates that the set of estimated response functions are valid, not only over a range of frequencies and amplitudes of the input signal, but are also valid when used with an entirely different input signal (random noise compared to sinusoidal).

The above examples have demonstrated that the response functions estimated in the chaotic region can accurately predict the behaviour in the bifurcation and linear regions of the oscillator. This would not be the case if the different regions were governed by different families of solutions. The estimated response functions represent a local single valued solution to the motion of the charge carriers as the region of phase space where they may be appropriately used is quite broad. This indicates that the equation of motion of the charge carriers in the diode are governed by a sequence of nonlinear pulses or solitons [17,18], and not by the bifurcation or return map approaches.

CONCLUSIONS

In this work, a formalism, developed by the authors in companion papers, has been employed to estimate the linear and leading nonlinear response functions of a driven non-linear oscillator. The period doubling and chaotic behaviour reported by other investigators using circuits of this type have been replicated. The first and second order response functions were estimated from the time series moments of the input and output time series data collected from the circuit in a chaotic bifurcation mode or 'phase'. These estimated response functions were then employed to predict the output of the circuit, when driven with a range of

different frequencies and voltage amplitudes for a sinusoidal input signal, and for a stochastic input signal. The range of frequencies and voltage amplitudes applied to the circuit span a region of the phase space, from the chaotic phase, in which the response functions were estimated, through the period doubling sequence (x16 and lower bifurcation modes) to lower voltages, where the circuit's behaviour is approximately linear. In all cases the predicted output voltage of the system, using the estimated response functions, displayed good agreement between the measured and model predicted output time series. This work has demonstrated that a single set of response functions can characterise a wide region of the phase space of the circuit, and also that these estimated response functions are independent of the type of input signal used. This work indicates that the equation of motion of the charge carriers in the diode are governed by a sequence of nonlinear pulses or solitons [17,18], rather than by the bifurcation or return map approaches. This work has also shown that the time series of the output signal from the circuit within the fully developed chaos region when driven with a sinusoidal voltage signal, appears to be a non-stationary modulated sine wave rather than a stochastic or chaotic sequence. The area under the peaks of the spectrum, which is proportional to the power provided by the forcing function to maintain the motion of the charge carriers, has been used to imply that the bifurcation states exhibited by the circuit are energetically favorable to the motion of the charge carriers.

Overall this work has shown that the formalism [5,6] can estimate the response functions of a nonlinear electrical resonator circuit. It has thus demonstrated the ability of the formalism to estimate the set of response functions that characterise a system, and the applicability of the formalism and the input-output representation, known as the Volterra series, to a wide class of systems which exhibit nonlinear phenomena.

ACKNOWLEDGEMENTS

This work was funded by the Building Sub-Committee of the UK Science and Engineering Research Council. The authors are pleased to acknowledge the support and helpful comments of Brian Day of the University of Bristol in this project.

REFERENCES

- [1] Volterra V, Singli Integrali Lineari dei Moti spontanei a caratteristiche indipendenti, Atti Torino, 35, 1900, p186-192.
- [2] Volterra V, Theory of Functionals and of Integral and Integro-differential Equations, Dover, New York, 1959.
- [3] Wiener N, Response of a Nonlinear Device to Noise, MIT Radiation Laboratory Report N.o 165, 1942.
- [4] Wiener N, Nonlinear Problems in Random Theory, John Wiley, New York, 1958.
- [5] Irving AD, Dewson T and Hong G, Nonlinear Response Function Estimation I : Mixed order case, Submitted to J. Phys. A, 1992.

- [6] Dewson T and Irving AD, Nonlinear Response Function Estimation II : Isolated order case, Submitted to J. Phys. A, 1992.
- [7] Kraichnan RH, Irreversible Statistical Mechanics of Incompressible Hydrodynamic Turbulence, Phys. Rev. 109, 1958, p1407-1422.
- [8] Linsay PS, Period Doubling and Chaotic Behaviour in a Driven Anharmonic Oscillator, Phys. Rev. Lett. 47(19), 1981, p1349-1352.
- [9] Testa J, Perez J and Jeffries C, Evidence for Universal Chaotic Behaviour of a Driven Nonlinear Oscillator, Phys. Rev. Lett. 48(11), 1982, p714-717.
- [10] Feigenbaum MJ, Quantitative Universality for a Class of Nonlinear Transformations, J. Stat. Phys. 19(1), 1978, p25-52.
- [11] Cascais J, Dilao R and Noronha Da Costa A, Chaos and Reverse Bifurcation in a RCL Circuit, Phys. Lett. 93A(5), 1983, p213-216
- [12] Baxter JH, Bocko MF and Douglass DH, Behaviour of a Nonlinear Resonator Driven at Subharmonic Frequencies, Phys. Rev. A, 41(2), 1990, p619-625.
- [13] Irving AD and Dewson T, Nonlinear Response Function Estimation : Moment Formulation and the Effect of Outliers, Submitted to J. Time Ser. Analysis, 1992.
- [14] Jackson EA, Perspectives of Nonlinear Dynamics Vol 1, Cambridge University Press, Cambridge, 1989, and Vol 2, 1990.
- [15] Van Buskirk R and Jeffries C, Observation of Chaotic Dynamics of Coupled Nonlinear Oscillators, Phys. Rev. A, 31(5), 1985, p3332-3357.
- [16] Irving AD and Dewson T, Nonlinear Response Function Estimation IV : Chaos and Nonlinear Auto-Regression, In preparation.
- [17] Toda M, Studies of a Nonlinear Lattice, Phys. Rep. 18C, 1975, p1-124.
- [18] Klinker T, Meyer-Ilse W and Lanterborn W, Period Doubling and Chaotic Behaviour in a Driven Toda Oscillator, Phys. Lett., 101A(8), 1984, p371-375.

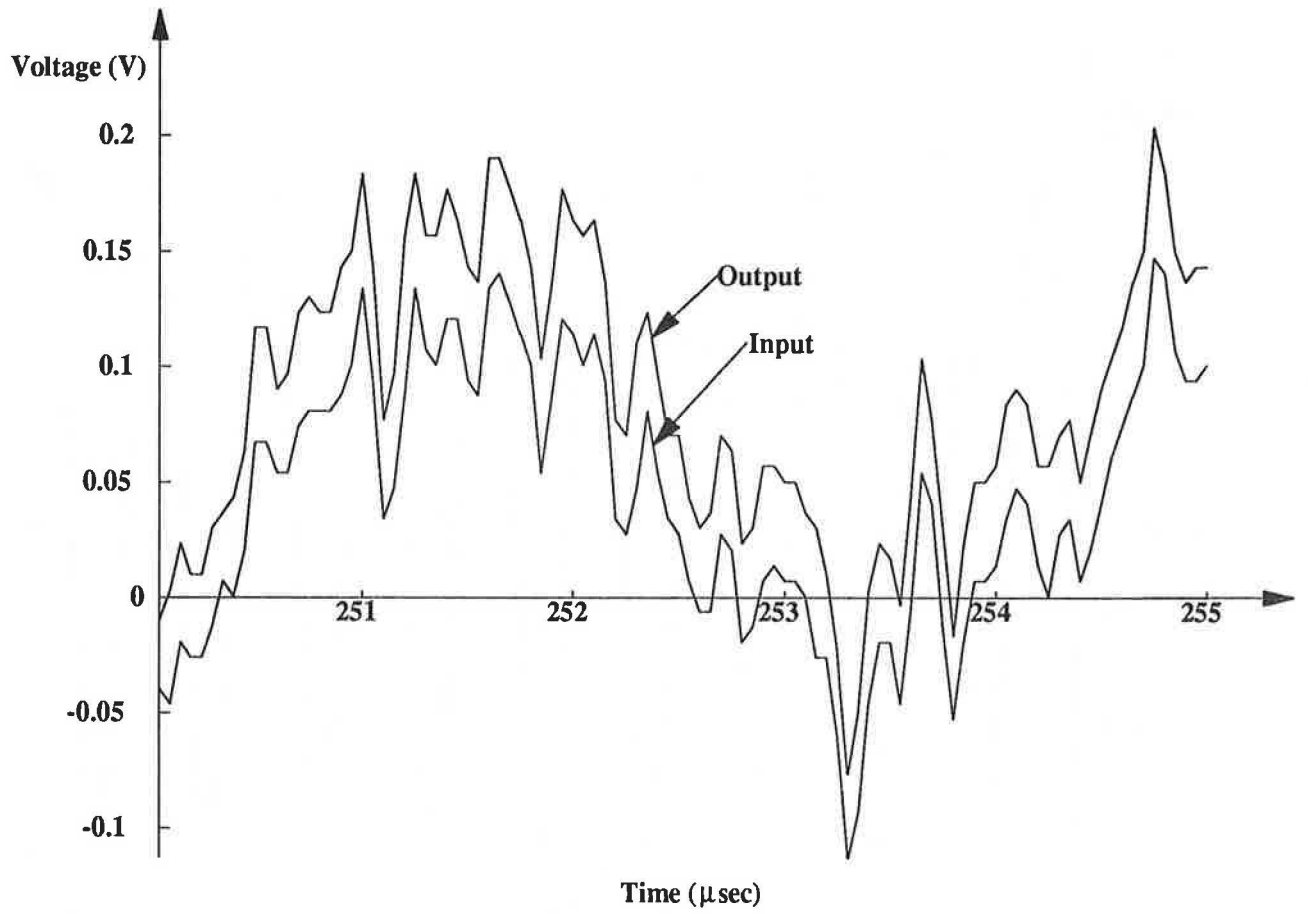


Figure 1 : A sample of the input voltage to and the output voltage from the circuit, when the circuit was driven by the noise source

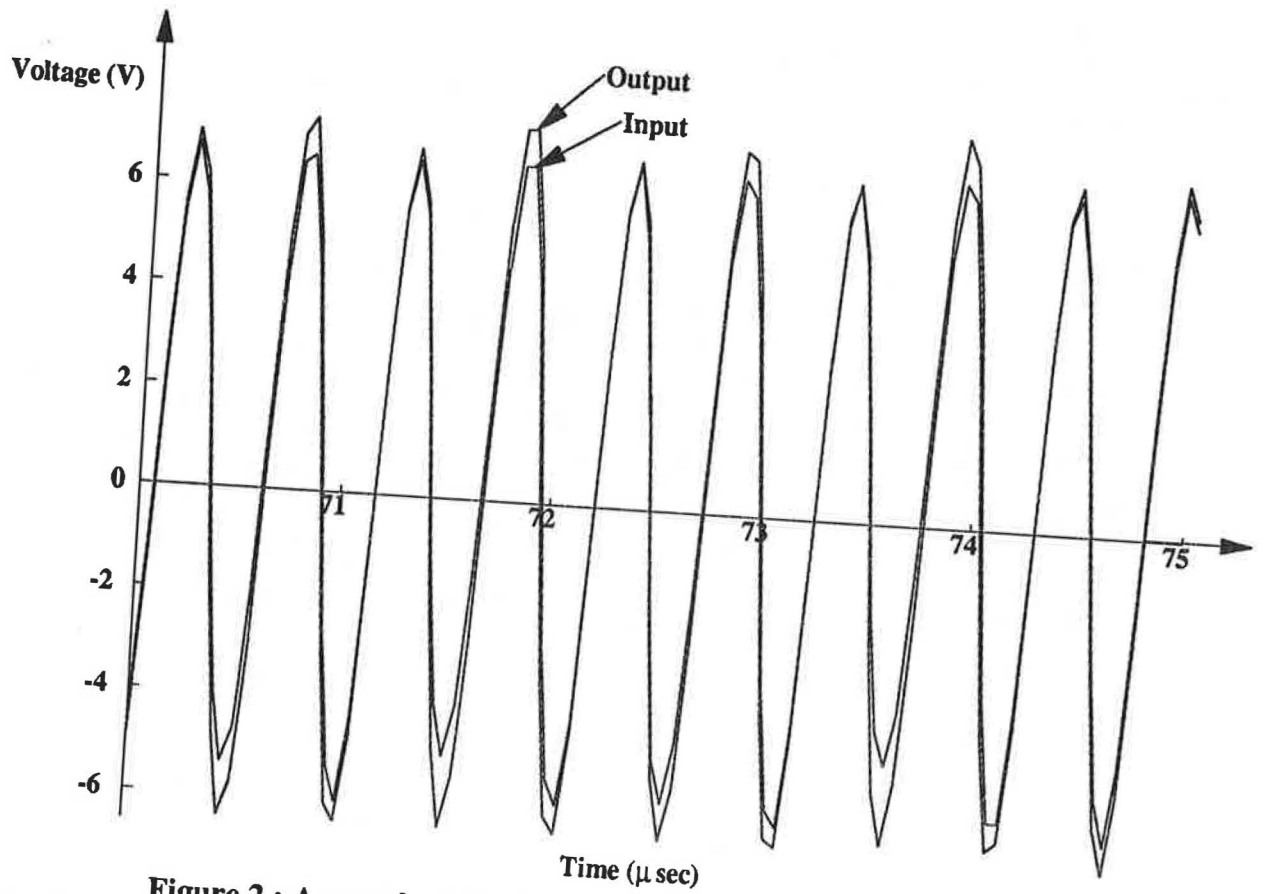


Figure 2 : A sample of the input voltage to and the output voltage from the circuit in the fully developed chaotic mode exhibited by the circuit, when the frequency of the driving voltage = 1.95 MHz

Figure 3 : The spectral density of the output voltage from the circuit, in the fully developed chaotic mode exhibited by the circuit, when the frequency of the driving voltage = 1.95 MHz

Figure 5 : The spectral density of the output voltage from the circuit, displaying the x2, x4, x8 and x16 bifurcations modes exhibited by the circuit when the frequency of the driving voltage = 1.79 MHz

Figure 8 : The spectral density of the output voltage from the circuit displaying the x2 bifurcation mode exhibited by the circuit when the frequency of the driving voltage = 1.08 MHz

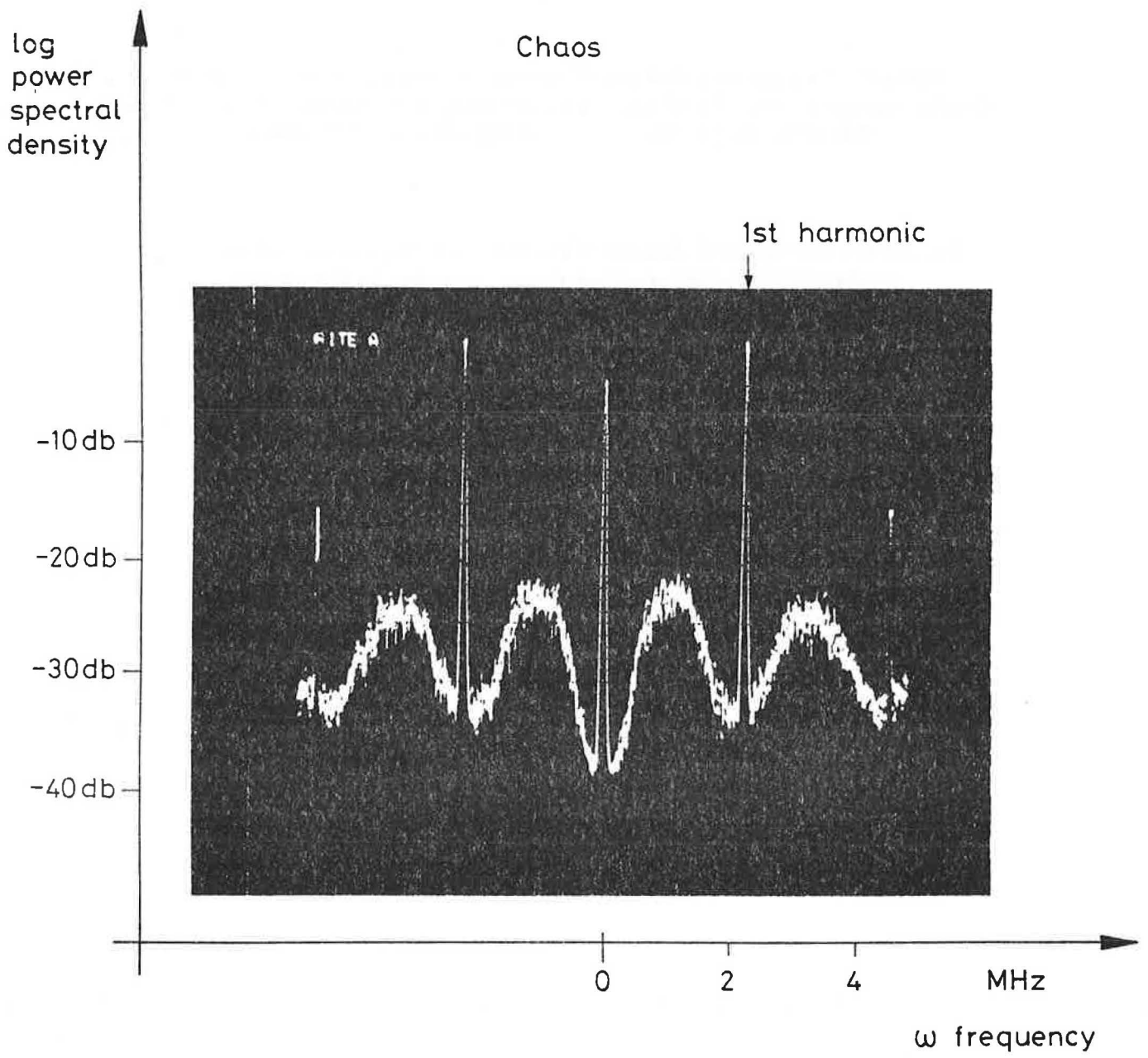


fig 3

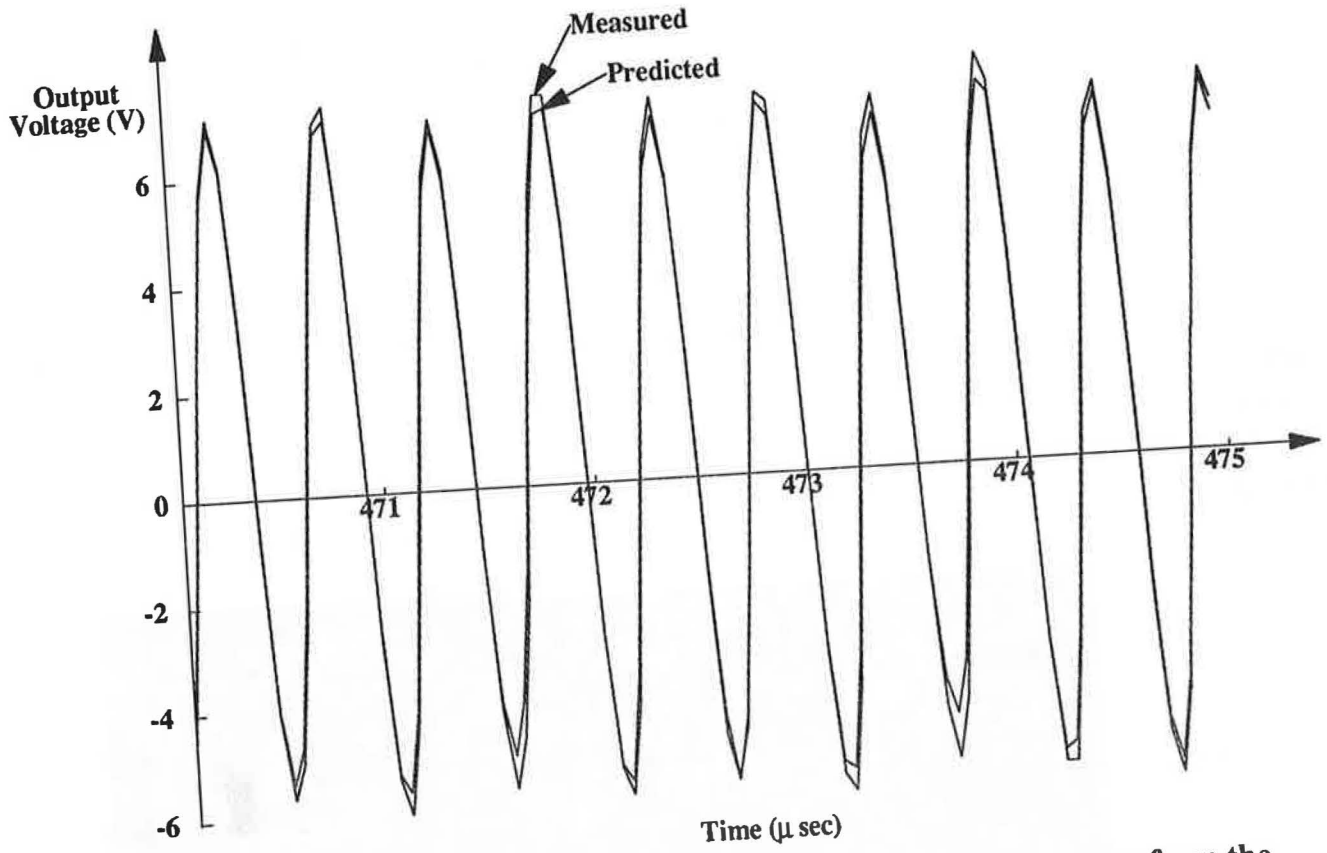


Figure 4 : A sample of the measured and predicted output voltage from the circuit in the fully developed chaotic mode exhibited by the circuit, when the frequency of the driving voltage = 1.95 MHz

x16 period doubling

log
power
spectral
density

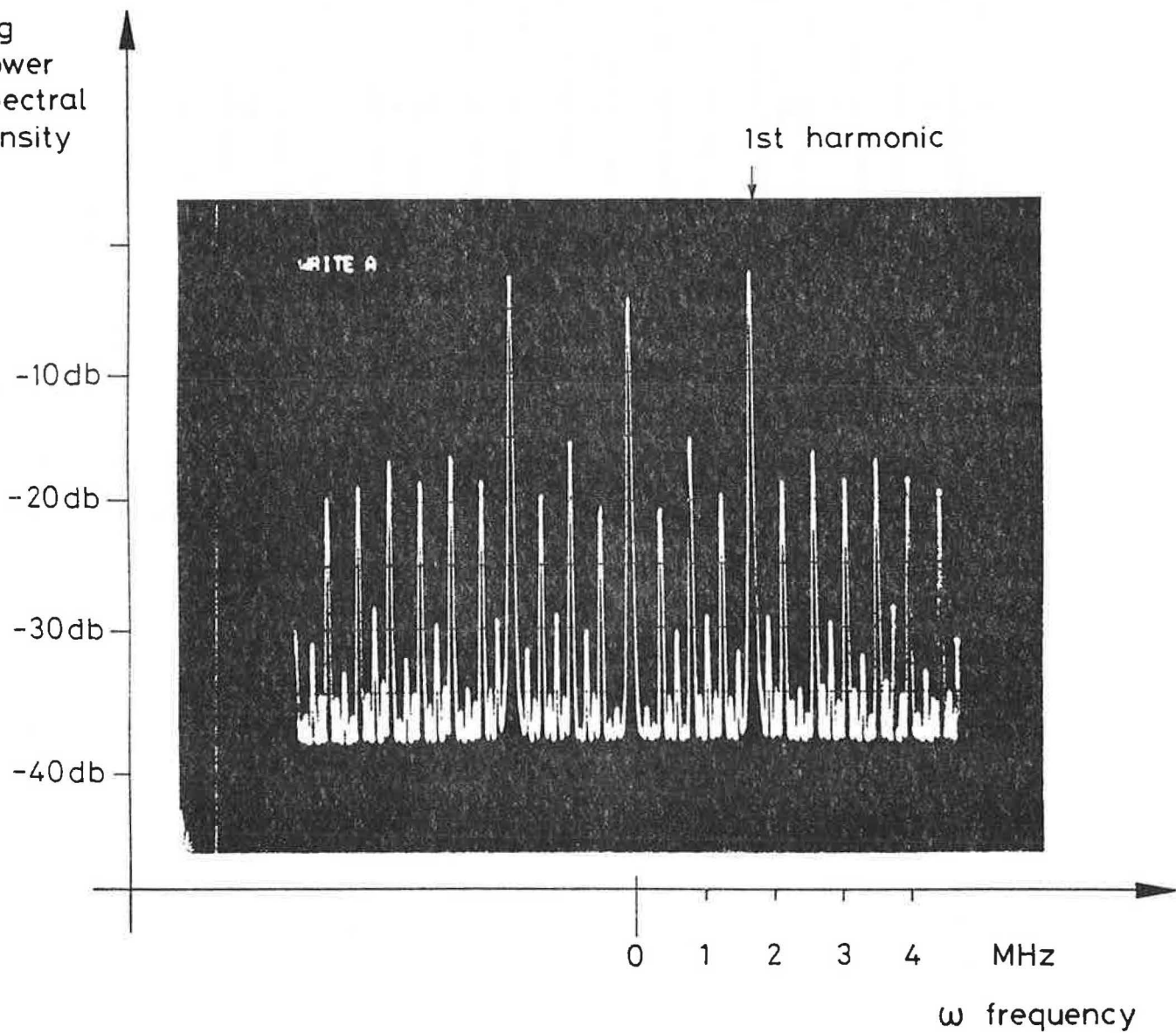


fig 5

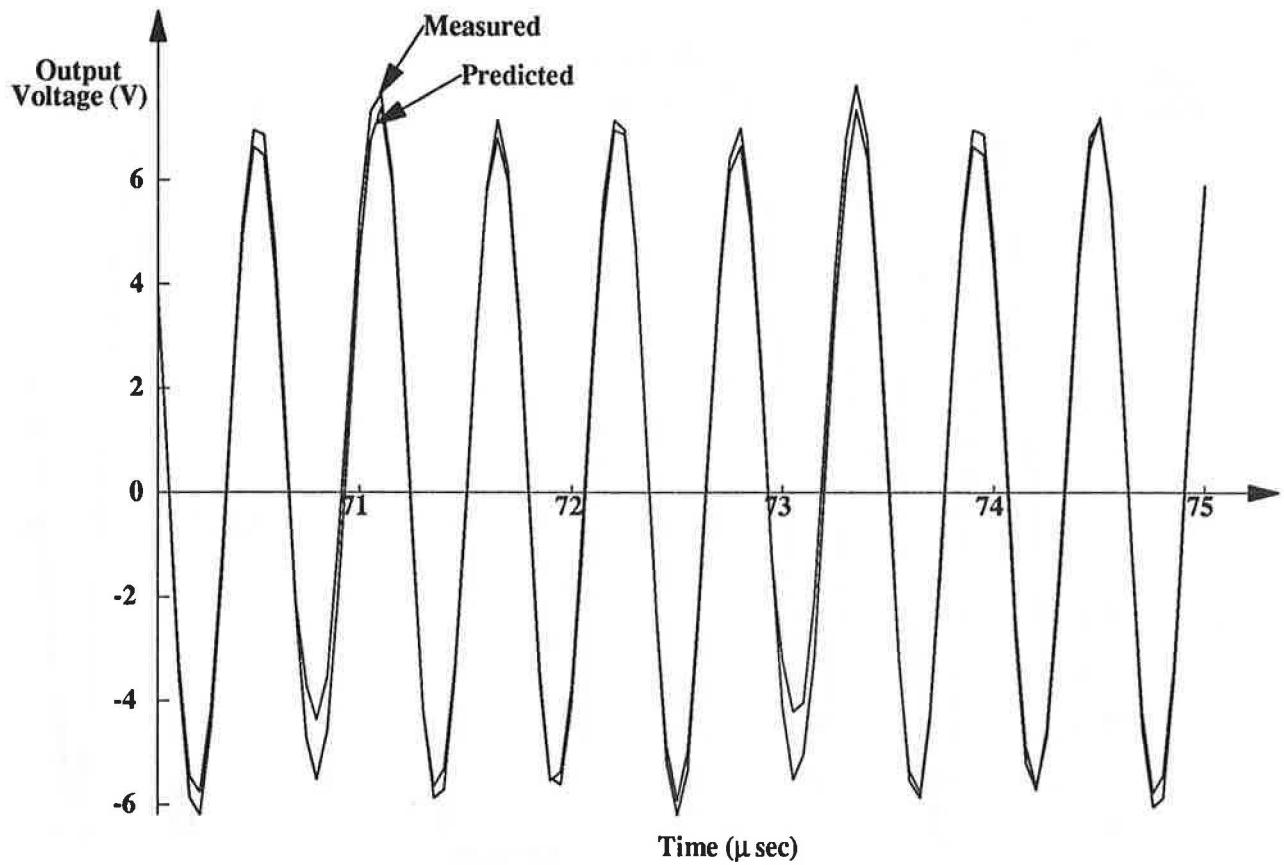


Figure 6 : A sample of the measured and predicted output voltage from the circuit at the saturation point of the x16 period bifurcations exhibited by the circuit, when the frequency of the driving voltage = 1.79 MHz

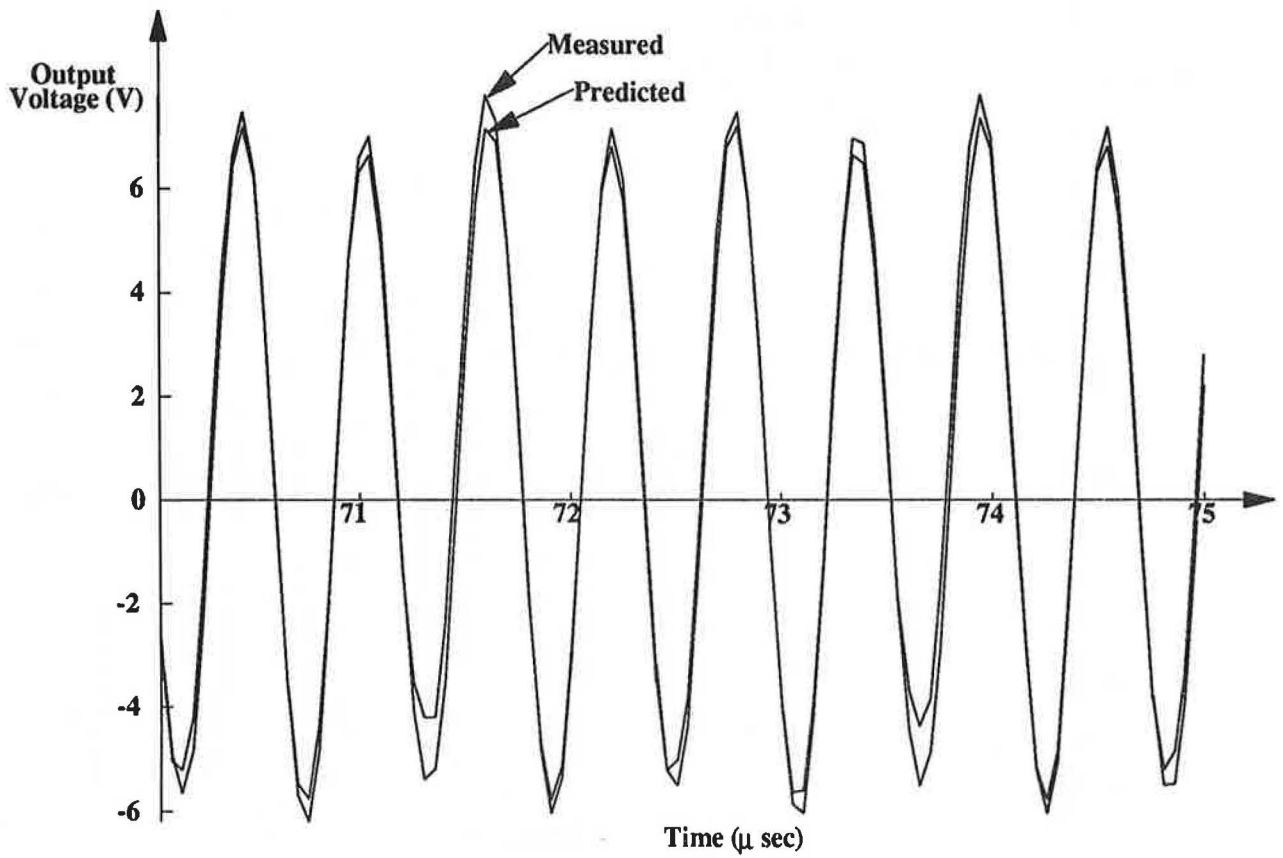
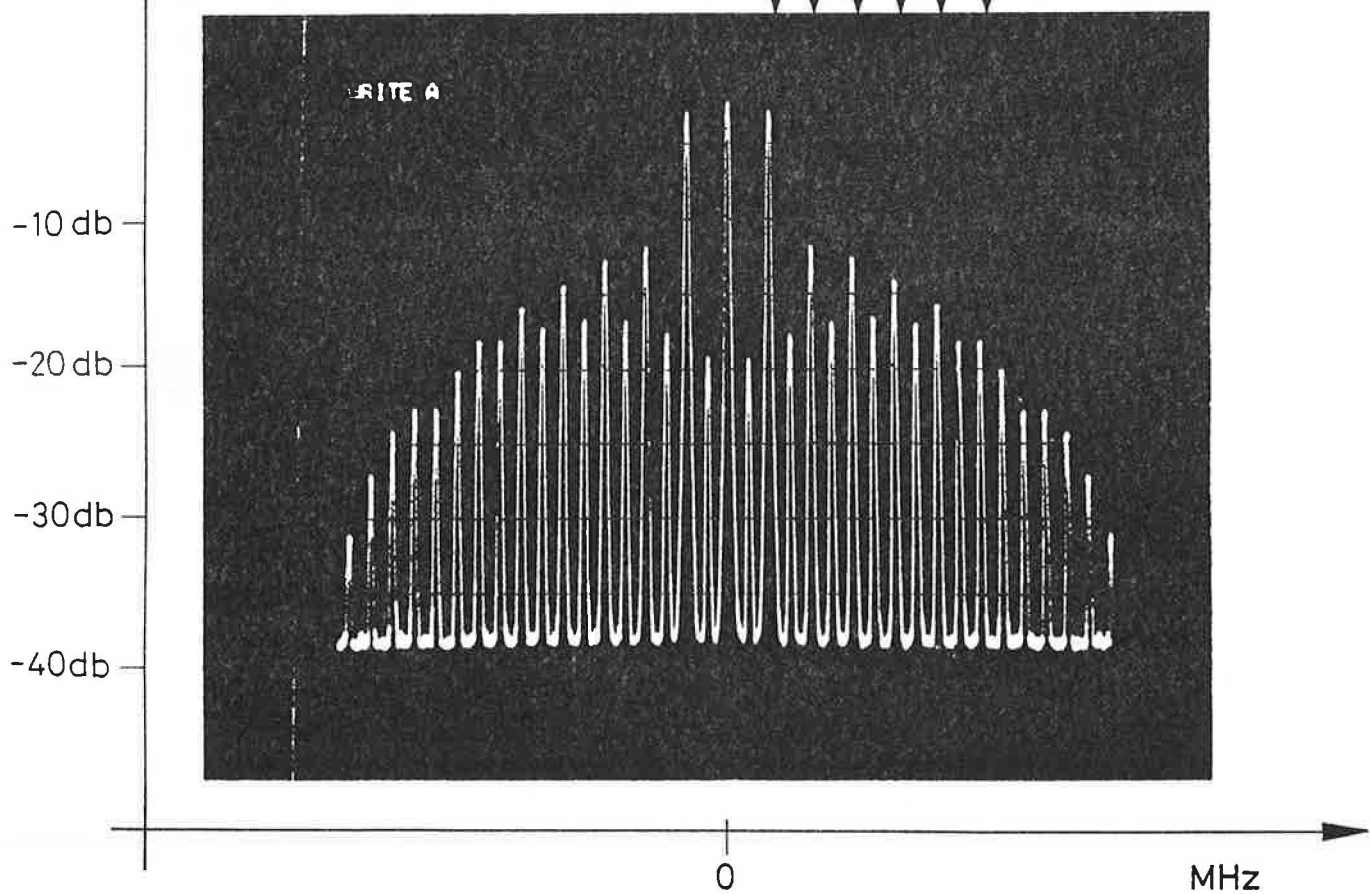


Figure 7 : A sample of the measured and predicted output voltage from the circuit at the saturation point of the x4 period bifurcations exhibited by the circuit, when the frequency of the driving voltage = 1.73 MHz

log
power
spectral
density

x2 period doubling

1 2 3 4 5 6 harmonics



f₀ 8

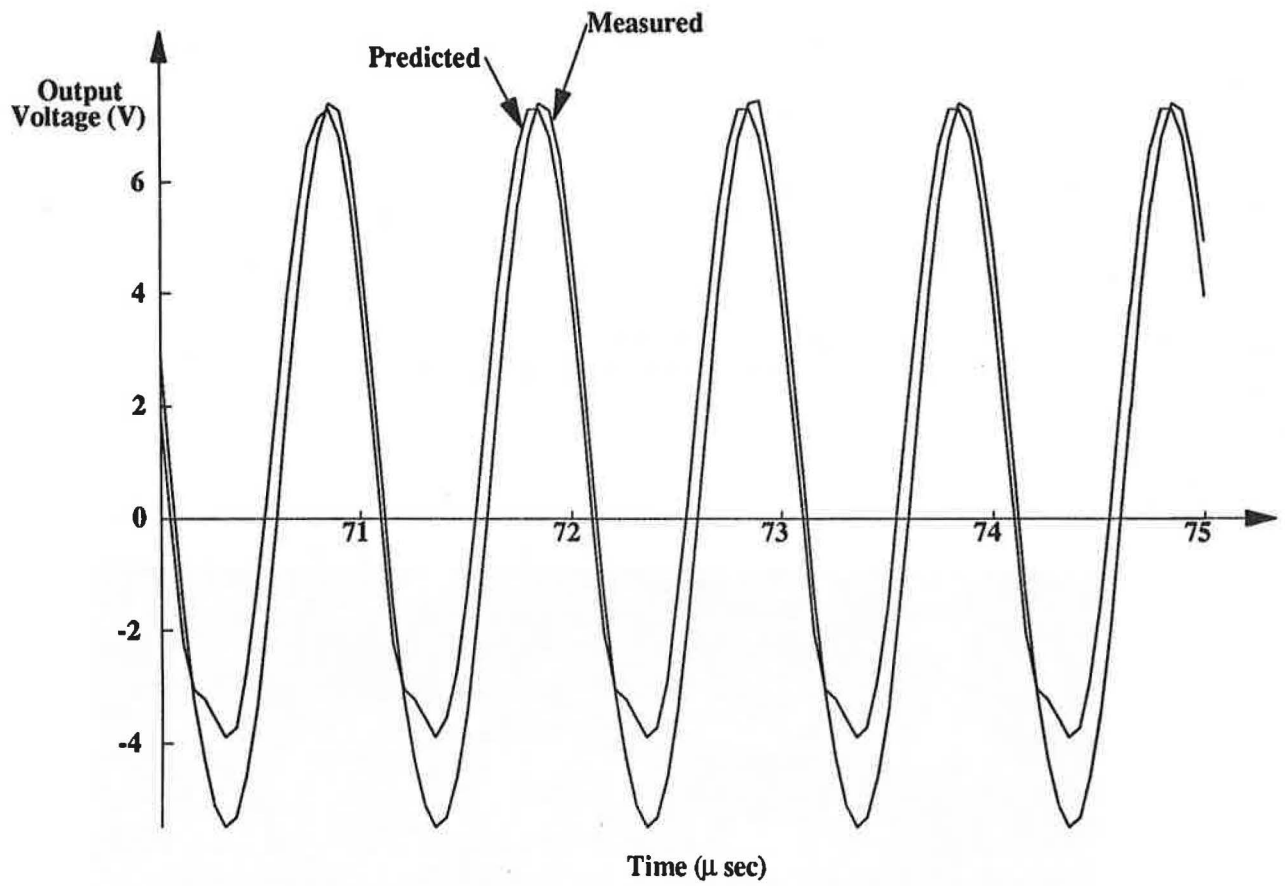


Figure 9 : A sample of the measured and predicted output voltage of the circuit, when the frequency of the drive voltage = 1 MHz

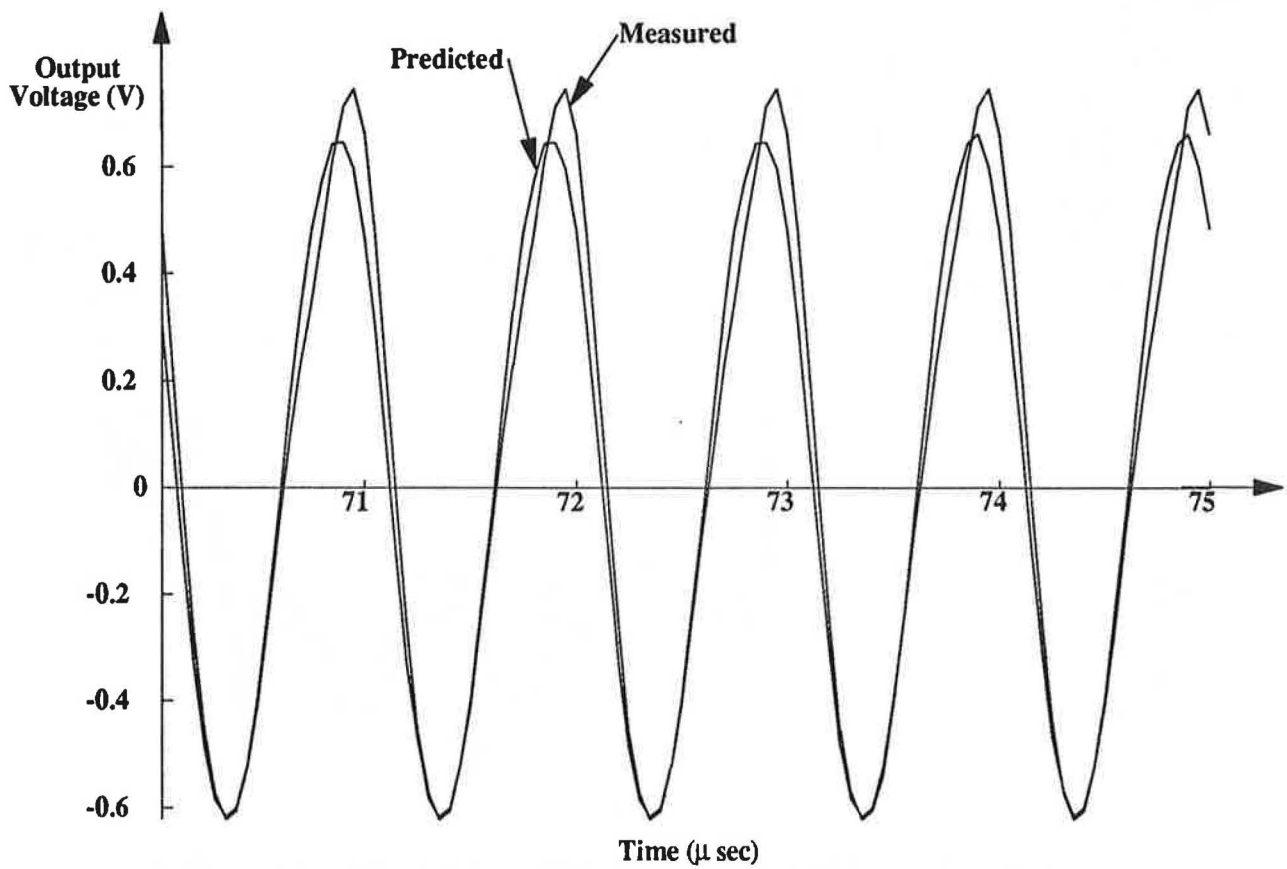


Figure 10 : A sample of the measured and predicted output voltage of the circuit, when the frequency of the drive voltage = 1 MHz

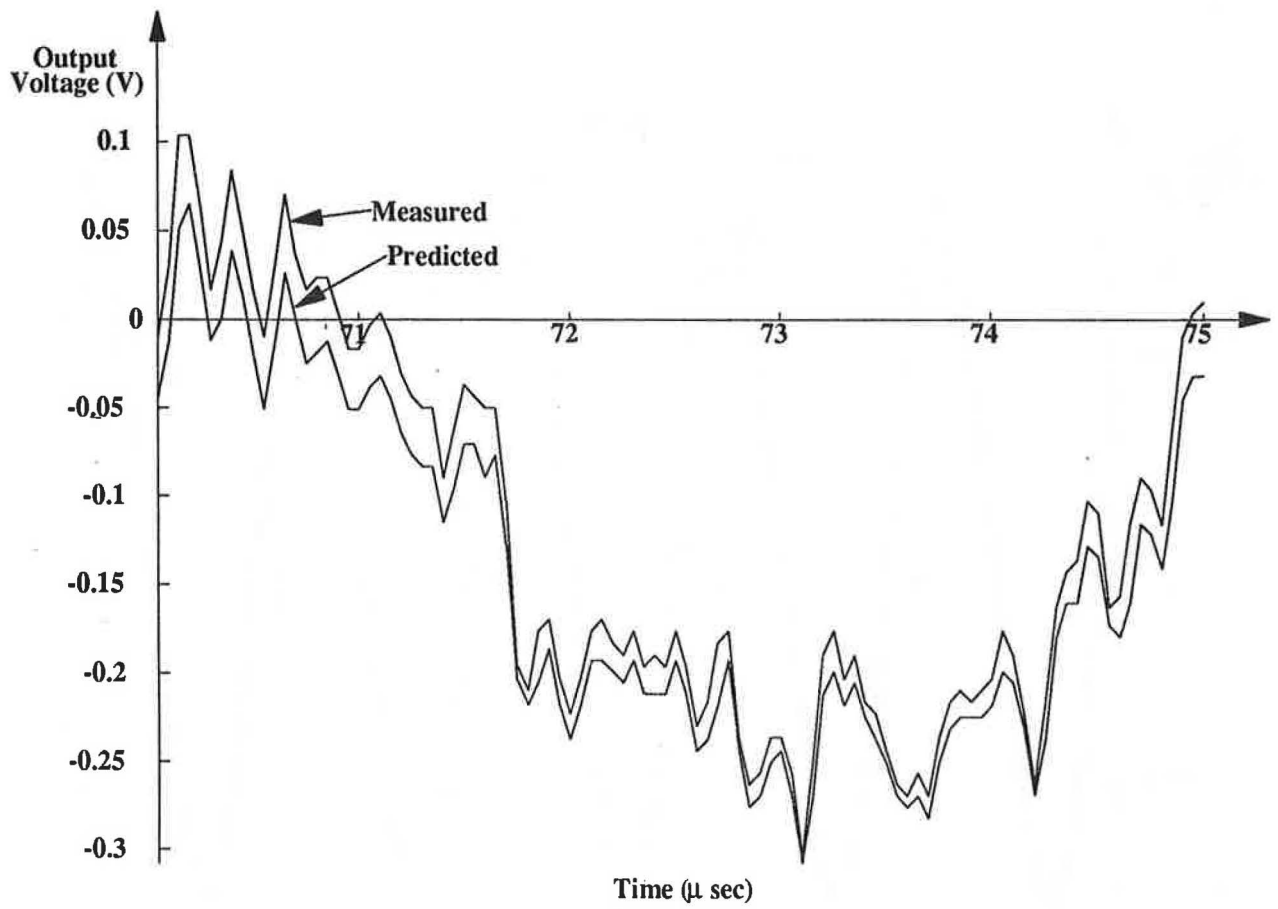


Figure 11 : A sample of the measured and predicted output voltage of the circuit, when the circuit was driven by a noise source

